Phosphatidylinositol 4,5-bisphosphate (PIP_2) stimulates the electrogenic Na/HCO_3 cotransporter NBCe1-A expressed in *Xenopus* oocytes

Jianping Wu[a], Carmel M. McNicholas[a], and Mark O. Bevensee[a,b,c,d,1]

[a]Department of Physiology and Biophysics, [b]Nephrology Research and Training Center, [c]Center of Glial Biology in Medicine, and [d]Civitan International Research Center, University of Alabama at Birmingham, Birmingham, AL 35294

Communicated by Gerhard Giebisch, Yale University School of Medicine, New Haven, CT, June 11, 2009 (received for review December 8, 2008)

Bicarbonate transporters are regulated by signaling molecules/ions such as protein kinases, ATP, and Ca^{2+}. While phospholipids such as PIP_2 can stimulate Na-H exchanger activity, little is known about phospholipid regulation of bicarbonate transporters. We used the patch-clamp technique to study the function and regulation of heterologously expressed rat NBCe1-A in excised macropatches from *Xenopus laevis* oocytes. Exposing the cytosolic side of inside-out macropatches to a 5% CO_2/33 mM HCO_3^- solution elicited a mean inward current of 14 pA in 74% of macropatches attached to pipettes ($-V_p = -60$ mV) containing a low-Na^+, nominally HCO_3^--free solution. The current was 80–90% smaller in the absence of Na^+, approximately 75% smaller in the presence of 200 μM DIDS, and absent in macropatches from H_2O-injected oocytes. NBCe1-A currents exhibited time-dependent rundown that was inhibited by removing Mg^{2+} in the presence or absence of vanadate and F^- to reduce general phosphatase activity. Applying 5 or 10 μM PIP_2 (diC8) in the presence of HCO_3^- induced an inward current in 54% of macropatches from NBC-expressing, but not H_2O-injected oocytes. PIP_2-induced currents were HCO_3^--dependent and somewhat larger following more NBCe1-A rundown, 62% smaller in the absence of Na^+, and 90% smaller in the presence of 200 μM DIDS. The polycation neomycin (250–500 μM) reduced the PIP_2-induced inward current by 69%; spermine (100 μM) reduced the current by 97%. Spermine, poly-D-lysine, and neomycin all reduced the baseline HCO_3^--induced inward currents by as much as 85%. In summary, PIP_2 stimulates NBCe1-A activity, and phosphoinositides are regulators of bicarbonate transporters.

acid-base | bicarbonate | pH | phosphatase | phospholipid

Na-coupled HCO_3^- transporters play important roles in intracellular pH (pH_i) regulation and ion transport in many tissues. Since the expression cloning of the first cDNA encoding a cation-coupled HCO_3^- transporter (NBCe1) from salamander kidney (1), investigators have cloned by homology and characterized the function of additional electrogenic and electroneutral NBCs, cation-coupled anion exchangers, and associated splice variants (2). NBCe1 has 3 variants (A, B, and C) that differ at their amino and/or carboxyl termini. Na-coupled HCO_3^- transporters in conjunction with anion exchangers (AEs) are members of a superfamily of bicarbonate transporters (BTs).

The pH field is now poised to address new questions regarding the physiologic importance of numerous BTs. We hypothesize that proper pH_i regulation and ion transport require multiple BTs—each one playing a specific role under different physiologic conditions or regulatory stimuli. Classic signaling molecules, such as PKA/cAMP, PKC, Ca^{2+}, and ATP, can modulate heterologously expressed NBCe1. Investigators have reported that phosphorylation by activated PKA (3, 4) or an increase in cytosolic Ca^{2+} (5) can change the Na:HCO_3^- stoichiometry of the transporter. In addition, both cAMP (3) and ATP (6) appear to stimulate an NBC-mediated current, whereas PKC isoforms inhibit transporter activity (7).

Other binding proteins or NBC domains can regulate transporter function. For NBCe1, the unique amino terminus of the A variant stimulates activity, whereas the different amino terminus of the B and C variants inhibits activity (8). Such automodulation may involve additional binding proteins and signaling molecules. Indeed, Shirakabe et al. (9) reported that the IP_3 receptor binding protein released with IP_3 (IRBIT) can stimulate NBCe1-B co-expressed in oocytes by binding to the transporter's amino terminus and masking an autoinhibitory domain.

Very little is known about the influence of phospholipids on the activity of BTs. PIP_2 is noteworthy because in addition to its classic role as a precursor of the Ca^{2+}-mobilizing inositol triphosphate (IP_3) and the kinase-activating diacylglycerol (DAG), the phosphoinositide is a signaling molecule that can regulate solute movement (10). In pioneering work, Hilgemann and Ball (11) found that PIP_2 directly stimulates both the cardiac Na-Ca exchanger and K_{ATP} channel. Phosphoinositides also regulate the activity of acid-base transporters. For example, PIP_2 is required for optimal activity of NHE1 transfected into an AP-1 cell line (12), and can rescue reduced NHE1 activity elicited by depleting ATP in Chinese hamster ovary (CHO) fibroblasts (13). Furthermore, the phosphoinositide PIP_3 stimulates NHE3 in opossum kidney cells, but not NHE1 in the CHO cells (13). We hypothesize that phospholipid regulation of BTs is also diverse, and can influence the acid-base physiology of kidney, brain, and other organ systems.

In the present study, we used the patch-clamp technique to examine the effect of cytosolic PIP_2 on the activity of electrogenic NBCe1 in excised inside-out macropatches from oocytes heterologously expressing rat NBCe1-A. Applying bath HCO_3^- elicited a DIDS-sensitive, Na^+-dependent inward current that exhibited rundown. Cytosolic PIP_2 reduced the rate of rundown and stimulated an inward current in the presence but not absence of bath HCO_3^-. The PIP_2 stimulation was inhibited by removing bath Na^+ or applying either DIDS or polyanionic charge screeners. PIP_2 therefore stimulates the activity of NBCe1-A.

Portions of this work have been published in preliminary form (14).

Results

Electrogenic NBCe1-A Activity in Excised Macropatches. We previously reported that applying bath HCO_3^- to create symmetrical Na^+ and HCO_3^- gradients across inside-out macropatches ($-V_p = -60$ mV) from NBC-expressing oocytes elicited small DIDS-reversible inward currents (8). Here, we stimulated these currents by increasing the Na^+ and HCO_3^- gradients using a nominally HCO_3^--free pipette solution containing low (10 mM) Na^+. As shown in Fig. 1*A*, switching the bath (cytosolic) side of the patch from the nominally HCO_3^--free ND96 solution to one containing 5% CO_2/33 mM HCO_3^- elicited a pronounced inward current (*a*), which was revers-

Author contributions: J.W., C.M.M., and M.O.B. designed research; J.W. performed research; J.W., C.M.M., and M.O.B. analyzed data; and J.W., C.M.M., and M.O.B. wrote the paper.

The authors declare no conflict of interest.

[1]To whom correspondence should be addressed. E-mail: bevensee@physiology.uab.edu.

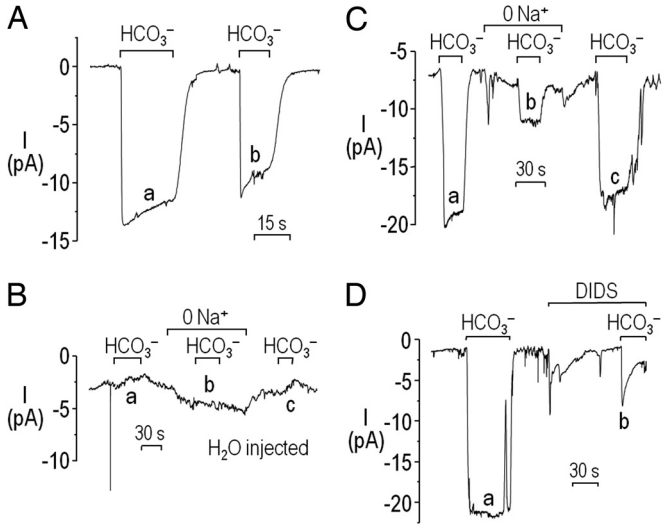

Fig. 1. Electrogenic NBCe1-A activity in macropatches. Experiments were performed on inside-out macropatches ($-V_p = -60$ mV) excised from oocytes expressing rat NBCe1-A or injected with H_2O. (*A*) HCO_3^--dependence. Switching from ND96 to a 5% CO_2/33 mM HCO_3^- solution elicited inward currents (*a* and *b*) that exhibited rundown. (*B*) Macropatch from a H_2O-injected oocyte. Applying CO_2/HCO_3^- in either the presence of bath (cytosolic) Na^+ (*a* and *c*) or absence of bath Na^+ (*b*) did not elicit appreciable currents. (*C*) Na^+ dependence. The HCO_3^--induced currents (*a* and *c*) were smaller in the absence of bath Na^+ (*b*). (*D*) DIDS sensitivity. The HCO_3^--induced current (*a*) was smaller and transient in the presence of 200 μM DIDS in the bath solution (*b*).

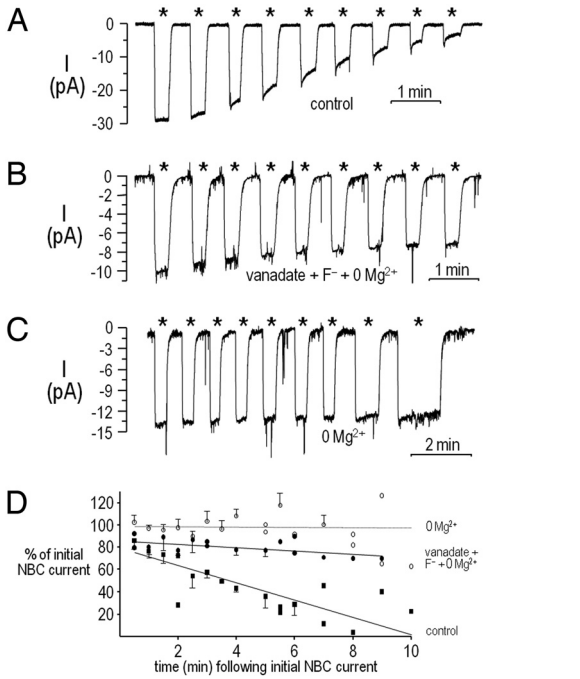

Fig. 2. Sensitivity of NBCe1-A rundown to general phosphatase inhibition. Experiments were performed on inside-out macropatches ($-V_p = -60$ mV) excised from oocytes expressing NBCe1-A. (*A*) Repetitive HCO_3^--induced inward currents under control conditions. Inward currents became progressively smaller in magnitude and decayed faster with subsequent HCO_3^--induced activations (*). The magnitude of the initial HCO_3^--induced NBC current was particularly large in this experiment. (*B*) Repetitive HCO_3^--induced inward currents under conditions that inhibited general phosphatase activity. Rundown was less in the simultaneous absence of Mg^{2+} and presence of 5 mM F^- and 100 μM vanadate. (*C*) Repetitive HCO_3^--induced inward currents in the absence of Mg^{2+}. Rundown was also less in the absence of Mg^{2+}. (*D*) Summary data from experiments shown in panels *A*–*C*. HCO_3^--induced currents normalized to the initial HCO_3^--induced current are plotted as a function of time (in 30 s intervals) with constant or successive exposures to CO_2/HCO_3^- for patches under control conditions (■), in the simultaneous absence of Mg^{2+} and presence of F^- and vanadate (●), or in the absence of Mg^{2+} (○). $n \geq 3$ for symbols with error bars, otherwise $n = 1$.

ible. The inward current is consistent with NBC-mediated net-negative charge moving from bath to pipette. NBCe1-A currents typically decayed after activation (*a*), and often became smaller with repetitive activation (compare *b vs. a*). These 2 observations are consistent with "rundown" of NBCe1-A activity (see next section). In 74% of patches, we observed a mean HCO_3^--induced inward current of 14 ± 1 pA ($n = 201$). In the remaining patches, HCO_3^--induced currents were not appreciable (≤ 0.5 pA). As shown in Fig. 1*B*, HCO_3^--induced currents in patches from H_2O-injected oocytes were not observed either in the presence (*a* and *c*) or absence (*b*) of Na^+. Similar results (in the presence of Na^+ and HCO_3^-) were obtained in 45 control macropatches. The small inward current elicited by removing bath Na^+ in Fig. 1*B* is consistent with a small endogenous Na^+ conductance.

We next examined the ion dependence of the HCO_3^--induced inward current. As shown in Fig. 1*C*, the HCO_3^--induced inward current (*a* and *c*) was approximately 75% less when Na^+ was replaced with Li^+ (*b*); the mean current was 80 ± 3% less ($n = 14$). Similar results were obtained with $NMDG^+$ as the Na^+ substitute and in the absence of external Mg^{2+} to reduce the rate of rundown (see next section). The mean current was 90 ± 8% less with $NMDG^+$ as the Na^+ substitute ($n = 5$)—an inhibition no different than with Li^+ ($P = 0.20$).

Similar to other BTs, NBCe1 is inhibited by stilbene derivatives such as DIDS (6, 8, 15–17), which can inhibit NBCe1 from the intracellular side of the plasma membrane (6). As shown in Fig. 1*D*, the HCO_3^--induced inward current (*a*) was reduced approximately 76% when the NBC-expressing patch was exposed to 200 μM DIDS in the bath solution (*b*). In 4 such experiments, 200 μM DIDS inhibited the mean current by 75 ± 15% [similar to such inhibition in whole-cell oocyte experiments (16)]. As previously described (8), we also applied 200 μM DIDS after activating NBC with the HCO_3^- solution. In 12 patches exposed to solutions with or without Mg^{2+}, 200 μM DIDS reduced the HCO_3^--induced current by 78 ± 6%.

Rundown of NBCe1-A Activity in Excised Macropatches. NBCe1-A rundown shown in Fig. 1*A* is reminiscent of a phenomenon seen with channels such as ROMK and K_{ATP} (18–20) that is often due to a phosphatase-mediated dephosphorylation event. We therefore monitored NBC rundown in the simultaneous absence of Mg^{2+} and presence of 5 mM F^- and 100 μM vanadate (0 Mg^{2+}/F^-/vanadate)—a condition that inhibits broad-spectrum phosphatase activity. Successive HCO_3^- exposures in the presence of 2 mM Mg^{2+} led to rundown (Fig. 2*A*), which was markedly reduced by 0 Mg^{2+}/F^-/vanadate (Fig. 2*B*). As shown in Fig. 2*C*, removing Mg^{2+} alone also inhibited NBC rundown. From experiments similar to those shown in panels *A*–*C*, we plotted the magnitude of HCO_3^--induced currents as a function of time when patches were exposed or re-exposed to HCO_3^- (Fig. 2*D*). The best-fit line to the control data has a slope (−0.077 ± 0.010 min^{-1}, $n = 40$, 9 experiments) that is steeper ($P < 0.0001$) than obtained for the 0 Mg^{2+}/F^-/vanadate data (−0.015 ± 0.009 min^{-1}, $n = 29$, 5 experiments) or the 0 Mg^{2+} data (−0.001 ± 0.009 min^{-1}, $n = 73$, 21 experiments). The slopes of the linear fits to the 0 Mg^{2+}/F^-/vanadate and 0 Mg^{2+} data are no different ($P = 0.4$), although the *y*-intercept of the fit to the 0 Mg^{2+} data is significantly greater ($P < 0.0001$). The data are consistent with 1 or more Mg^{2+}-sensitive phosphatases inhibiting NBC activity through dephosphorylation of either NBCe1-A itself or other regulatory factors.

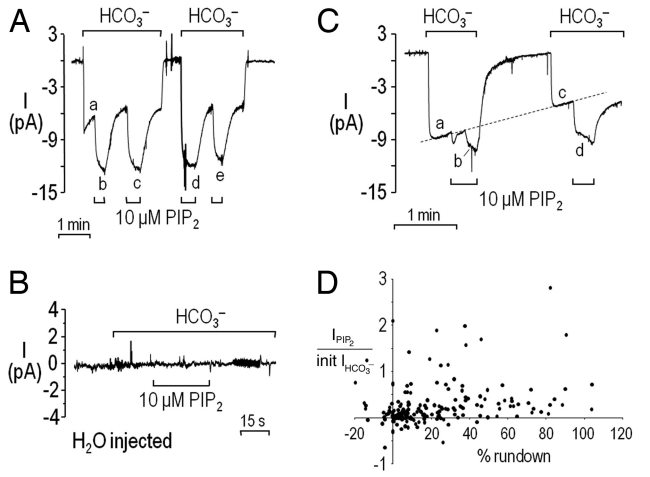

Fig. 3. PIP_2-induced stimulation of NBCe1-A. Experiments were performed on inside-out macropatches ($-V_p = -60$ mV) excised from oocytes expressing NBCe1-A or injected with H_2O. (*A*) NBCe1-A. Applying CO_2/HCO_3^- elicited an NBC-mediated inward current that decayed slowly (*a*). Adding 10 μM PIP_2 (C8 form) in the presence of HCO_3^- elicited an inward current that displayed minimal decay (*b*, *c*, and *e*). Applying CO_2/HCO_3^- and PIP_2 simultaneously had an additive effect (*d*). (*B*) H_2O control. Exposing the patch to the HCO_3^- solution and then PIP_2 had no effect on current. (*C*) NBCe1-A. Applying CO_2/HCO_3^- elicited an NBC-mediated inward current (*a*) that decayed during the experiment (current *c*). Adding 10 μM PIP_2 in the presence of HCO_3^- elicited an inward current that was larger with more rundown (*d vs. b*). (*D*) Summary data from experiments similar to those shown in panels *A* and *C*. The magnitude of PIP_2-induced currents (as a function of the initial HCO_3^--induced currents) is plotted as a percentage of rundown from the initial HCO_3^--induced currents. $n = 194$ from 156 experiments. The following 3 outliers are not plotted: 4.0 at -2.9% rundown, 5.2 at 78% rundown, and 5.7 at 91% rundown. In a small number of experiments, the rundown was negative because the current with the patch exposed to HCO_3^- increased somewhat during the experiment for unknown reasons.

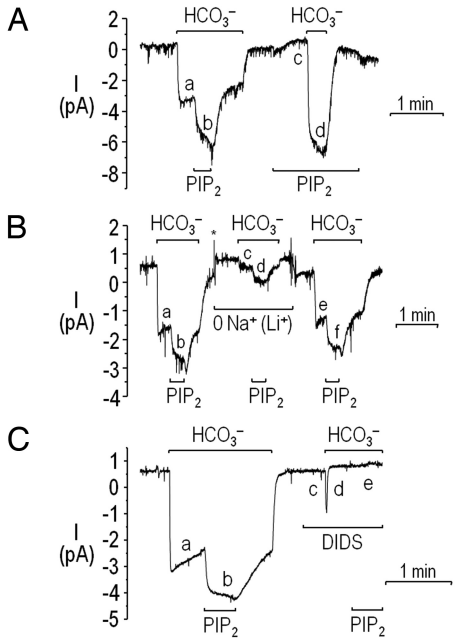

Fig. 4. Ion dependencies and pharmacology of the PIP_2-induced stimulation of NBCe1-A. Experiments were performed on inside-out macropatches ($-V_p = -60$ mV) excised from oocytes expressing NBCe1-A. (*A*) HCO_3^--dependence. Applying 10 μM PIP_2 in the presence of HCO_3^- or vice versa elicited a larger inward current (*b* and *d*) than seen with HCO_3^- alone (*a*). However, applying PIP_2 in the absence of HCO_3^- did not generate an appreciable current (*c*). (*B*) Na^+ dependence. The HCO_3^--induced inward current was smaller in the absence (*c*) vs. presence (*a* and *e*) of Na^+. In the presence of CO_2/HCO_3^-, the PIP_2-induced inward current was smaller in the absence (*d*) vs. presence (*b* and *f*) of Na^+. *noise spike truncated. (*C*) DIDS sensitivity. PIP_2 elicited an inward current (*b*) following the HCO_3^--induced current (*a*). In the presence of 200 μM DIDS [which had little effect in the nominal absence of HCO_3^- (*c*)], applying the HCO_3^- solution alone (*d*) or with PIP_2 (*e*) failed to elicit an appreciable current. Rundown was minimized by using Mg^{2+}-free solutions. As shown in all panels, PIP_2 reduced or inhibited the rundown following HCO_3^--induced activation.

PIP_2-induced Inward Currents in NBCe1-expressing Oocytes. Phosphatase-dependent NBCe1-A rundown may involve Mg^{2+}-dependent dephosphorylation of PIP_2. We therefore examined the effect of cytosolic PIP_2 (diC8 form) on NBCe1-A activity in the macropatch.

Exposing an NBC-containing macropatch to the 33-mM HCO_3^- solution elicited an inward current (*a*), which decayed slowly in the absence of phosphatase inhibitors (Fig. 3*A*). However, switching to the HCO_3^- solution containing 10 μM PIP_2 increased the inward current in a reversible manner and decreased rundown (*b*, *c*, and *e*). The HCO_3^-- and PIP_2-induced inward currents were additive (*d*). As shown in Fig. 3*B*, neither the HCO_3^- solution nor 10 μM PIP_2 in the HCO_3^- solution generated a current in a macropatch from a H_2O-injected control oocyte ($n = 13$). In 93 NBC-expressing macropatches exposed to HCO_3^- solutions containing either 2 or 3 mM Mg^{2+}, applying 5 or 10 μM PIP_2 induced an inward current (>0.5 pA) in 47 patches (51%), had no/minimal effect (0 ± 0.5 pA) in 29 patches (31%), and reduced the HCO_3^--induced inward current (<-0.5 pA) in 17 patches (18%). For experiments with PIP_2-induced inward currents, HCO_3^- elicited a mean current of 12.7 ± 2.5 pA, which decayed to a mean current of 10.3 ± 2.4 pA before applying 5 or 10 μM PIP_2. PIP_2 subsequently increased the mean current to 13.4 ± 2.6 pA ($P < 0.0001$, paired *t* test).

Similar PIP_2 results were obtained with macropatches exposed to phosphatase-inhibiting conditions (e.g., 0 Mg^{2+}, 0 Mg^{2+}/F^-/vanadate, or F^-/vanadate). In 60 such NBC-expressing macropatches, applying 5 or 10 μM PIP_2 elicited an inward current (>0.5 pA) in 35 patches (58%), had no/minimal effect (0 ± 0.5 pA) in 22 patches (37%), and reduced the HCO_3^--induced inward current (<-0.5 pA) in 3 patches (5%). For experiments with PIP_2-induced inward currents, HCO_3^- elicited a mean current of 11.7 ± 1.7 pA, which decayed to a mean current of 10.7 ± 1.9 pA before applying 5 or 10 μM PIP_2. PIP_2 subsequently increased the mean current to 13.9 ± 2.0 pA ($P < 0.0001$, paired *t* test). In summary, PIP_2 elicited an inward current in 54% of 153 total macropatches (phosphatase-inhibiting or -noninhibiting conditions).

The experiment shown in Fig. 3*C* is similar to that in Fig. 3*A* except more NBC rundown was present as evident by an initial HCO_3^--induced current (*a*) that gradually decayed (dashed line from *a* to *c*). Applying 10 μM PIP_2 induced a larger inward current following more rundown (*d* vs. *b*). From single and multiple PIP_2-pulse experiments, we plotted the normalized PIP_2-induced currents as a function of % rundown. As shown in Fig. 3*D*, PIP_2-induced inward currents were somewhat smaller with less rundown (<10%).

Ion Dependencies and Stilbene Sensitivity of PIP_2-induced Inward Currents. If PIP_2 stimulates NBCe1-A, then PIP_2-induced inward currents should require bath HCO_3^- and Na^+, and be inhibited by DIDS. As shown in Fig. 4*A*, applying the HCO_3^- solution elicited the expected NBC-mediated inward current (*a*), and the inward current was enhanced by applying 10 μM PIP_2 (*b*). However, applying PIP_2 in the ND96 solution did not elicit an appreciable current (*c*), which was converted into a pronounced inward current by adding the HCO_3^- solution (*d*). Similar results

were obtained in 2 other experiments. The PIP_2-induced inward current therefore requires bath HCO_3^-.

We also examined the Na^+ dependence of the HCO_3^--dependent, PIP_2-induced inward current (Fig. 4*B*). Exposing the macropatch to the HCO_3^- solution in the presence of bath Na^+ elicited inward currents (*a* and *e*) that were subsequently stimulated by 10 μM PIP_2 (*b* and *f*). However, the HCO_3^- solution in the absence of bath Na^+ (Li^+ as the substitute) elicited a smaller inward current (*c*) that was only weakly stimulated by the PIP_2 (*d*). Similar results were obtained with $NMDG^+$ as the Na^+ substitute. In summary, removing bath Na^+ decreased the mean PIP_2-induced inward current by 62 ± 11% ($n = 6$). Therefore, the majority of the PIP_2-induced inward current requires bath Na^+.

Finally, we examined the DIDS sensitivity of the Na^+- and HCO_3^--dependent, PIP_2-induced inward current (Fig. 4*C*). Exposing the macropatch to HCO_3^- elicited an inward current that decayed slowly (*a*). Subsequently applying 10 μM PIP_2 in the presence of HCO_3^- enhanced the inward current (*b*) in a reversible manner. As expected, the HCO_3^--induced inward current was reversed by returning the patch to ND96. Adding 200 μM DIDS in ND96 had no effect on the current (*c*). In the continued presence of DIDS, neither the HCO_3^- solution (*d*) nor the HCO_3^- solution containing PIP_2 (*e*) elicited an appreciable current. In a total of 6 macropatch experiments, 200 μM DIDS inhibited the PIP_2-induced inward current by 90 ± 8%. In 2 of these experiments, DIDS was first applied to the ND96 solution (see Fig. 4*C*); in the other 4 experiments, DIDS was first applied to the HCO_3^- solution. Thus, DIDS inhibits the PIP_2-induced inward current.

Polycation Sensitivity of both PIP_2 Stimulation and Baseline Activity of NBCe1-A. PIP_2 typically binds to a stretch of positively charged amino acids (lysines and arginines) in a pleckstrin homology (PH) domain of a target protein such as ENaC (21). Polycations such as neomycin, polylysine, and the polyamine spermine can bind and neutralize the anionic headgroup of PIP_2, thereby interfering with lipid-protein interactions. We examined the effect of several polycation molecules on the PIP_2-stimulated NBCe1-A current.

As shown in Fig. 5*A*, exposing the macropatch from an NBC-injected oocyte to HCO_3^- elicited the expected inward current that decayed slowly due to rundown (*a*). Applying 10 μM PIP_2 in the presence of HCO_3^- stimulated NBC activity and inhibited rundown (*b*). NBC activity was completely blocked by simultaneously adding 500 μM neomycin and removing PIP_2 (*bc*). In the presence of neomycin, PIP_2 only elicited a small inward current (*cd*). After removing the neomycin, PIP_2 again elicited an inward current (*e*), which was inhibited again by re-adding neomycin (*f*). In 4 similar macropatch experiments, 250 or 500 μM neomycin inhibited the PIP_2-induced inward current by 69 ± 3%, and the inhibition was only partially reversible. Similar results were obtained in 2 experiments with 200 μg/mL poly-D-lysine (500–550 kDa), which nearly eliminated the PIP_2-induced current.

We performed a similar experiment using spermine (Fig. 5*B*). As expected, the HCO_3^--induced inward current that subsequently decayed (*a*) was stimulated by applying 10 μM PIP_2 (*b*). After returning the patch to ND96, the current returned to baseline (*c*). Applying 100 μM spermine elicited a small sustained outward current (*d*). With the patch in the continued presence of spermine, the HCO_3^- solution alone (*e*) or with PIP_2 (*f*) failed to induce an appreciable current. In 4 similar macropatch experiments, 100 μM spermine inhibited the PIP_2-induced inward current by 97 ± 10%.

Inhibition of the HCO_3^--induced inward current by both neomycin (Fig. 5*A*, *c*) and spermine (Fig. 5*B*, *e*) is consistent with endogenous PIP_2 promoting NBCe1 activity. We next examined the effect of these polycations, as well as poly-D/L-lysine, on the

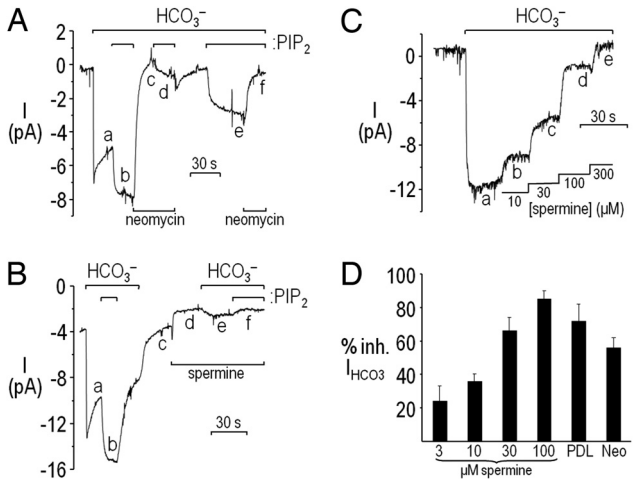

Fig. 5. Polycation sensitivity of both PIP_2 stimulation and baseline activity of NBCe1-A. Experiments were performed on inside-out macropatches ($-V_p = -60$ mV) excised from oocytes expressing NBCe1-A. (*A*) Sensitivity of PIP_2-induced stimulation to neomycin. The PIP_2-induced inward current was smaller in the presence (*d*) vs. absence (*b* and *e*) of 500 μM neomycin. Furthermore, inward currents were completely inhibited by neomycin (*c* and *f*). (*B*) Sensitivity of PIP_2-induced stimulation to spermine. PIP_2 stimulated the HCO_3^--induced inward current (*ab*). Returning the patch to ND96 caused the current to return to baseline (*c*). In the presence of spermine, which only elicited a small outward current (*d*), neither the HCO_3^- solution alone (*e*), nor one containing PIP_2 (*f*) elicited any appreciable current. (*C*) Sensitivity of the HCO_3^--induced current to spermine. Progressively higher concentrations of spermine from 10 to 300 μM (*b*-*e*) progressively inhibited the initial HCO_3^--induced current (*a*) to a greater extent. Rundown was minimized by using Mg^{2+}-free solutions. (*D*) Summary data of polycation-induced inhibition of inward currents elicited by CO_2/HCO_3^- (from panel *C*-type experiments). $n \geq 5$. In 2 experiments with 30 and 100 μM spermine, 30 μM spermine inhibited the entire HCO_3^--induced current; those data points were also included in the 100-μM group. Some data were obtained from experiments in which the polycation and HCO_3^- solution were applied simultaneously. PDL, poly-D-lysine; Neo, neomycin

NBC-mediated, HCO_3^--induced inward current. As shown in Fig. 5*C*, applying CO_2/HCO_3^- to a macropatch from an NBC-injected oocyte induced an inward current that decayed slowly in the absence of Mg^{2+} (*a*). Subsequently, applying progressively higher concentrations of spermine elicited progressively greater inhibition of the initial HCO_3^--induced current (*b*–*e*). In control experiments, 10 μM spermine did not elicit a current in CO_2/HCO_3^--exposed macropatches from H_2O-injected oocytes ($n = 5$). Poly-D-lysine (20 μg/mL; 6 out of 7 experiments), as well as 250 or 500 μM neomycin (12 out of 13 experiments) also inhibited HCO_3^--induced currents in macropatches from NBC-expressing oocytes. In other control experiments, poly-D-lysine ($n = 3$) or neomycin ($n = 4$) elicited small/no appreciable current in the absence of HCO_3^-. Inhibitory effects of the aforementioned polycations on the HCO_3^--induced current are summarized in Fig. 5*D*.

Discussion

Electrogenic NBCe1 Activity in Macropatches. The macropatch or "giant" membrane patch technique was originally developed for studies on electrogenic transporters, such as the cardiac Na-Ca exchanger (22), and was subsequently adapted for other applications, including ion channels (23). The Frömter laboratory has used both inside-out and outside-out configurations of the technique to examine sensitivity of rat NBCe1-A to cytosolic ATP (6) and Ca^{2+} levels (5). More recently, our group has used the inside-out configuration to characterize NBCe1 variants truncated at their amino termini (8). The technique provided 2

distinct advantages in the present study. First, we were able to control the solute composition on both sides of the membrane and apply PIP_2 directly to the cytoplasmic side. Second, we were able to measure NBC activity at high temporal resolution and identify transporter rundown.

We previously reported that HCO_3^--induced NBCe1-A currents are quite small (mean of ≈3.8 pA) with symmetrical Na^+ and HCO_3^- gradients across the macropatch held at −60 mV (cytosolic side). In the present study, we found that the mean current was enhanced approximately 3.7 fold (14 pA) by using a nominally HCO_3^--free, low-Na^+ pipette solution that increased the chemical driving force for NBC-mediated transport from bath to pipette. NBCe1-A transport activity was evident by a Na^+-dependent, DIDS-sensitive inward current elicited by applying a HCO_3^- solution to the cytosolic side of the macropatch. In a multi-HCO_3^- pulse experiment, the degree of NBC inhibition calculated from the reduced HCO_3^--induced current in the presence of an inhibitor or absence of Na^+ following a control HCO_3^--induced current will be an overestimate to the extent that any rundown is irreversible.

Regarding Na^+ dependence, we found a Na^+-independent component to the HCO_3^--induced inward current that was not seen in macropatches from H_2O-injected oocytes. The percentage of the NBC-mediated inward current that is Na^+ independent (10–20%) is similar to that seen in whole-cell voltage-clamp experiments (18%) where bath HCO_3^- drives NBC-mediated transport into oocytes (8). Further studies are required to determine if the Na^+-independent NBCe1-A current is due to transporter slippage (24) or a Na^+-independent (e.g., HCO_3^-) conductance. Channel-like behavior of NBCe1 might be similar to that reported for the electroneutral NBCn1, which exhibits Na^+ channel-like activity (25).

PIP_2-induced Stimulation of NBCe1 Activity. The PIP_2-induced inward current was due to NBC stimulation because the current required bath HCO_3^- and Na^+ and was inhibited by DIDS. Furthermore, applying polycation molecules that are known to screen the anionic headgroup of PIP_2 inhibited the PIP_2-induced current. It is worth noting that 38% of the PIP_2-induced inward current was Na^+ independent (Fig. 4*B*). The Na^+-independent current data are consistent with PIP_2 stimulating both transporter and any channel-like behavior of NBCe1.

The observation that PIP_2 stimulates NBCe1-A activity raises a couple of important questions. One question is: Does PIP_2 stimulate NBCe1 activity in an intact cell? We have recently injected PIP_2 directly into voltage-clamped oocytes expressing NBCe1 variants (-A, -B, and -C) that differ at their amino and/or carboxyl termini. Although all 3 variants exhibit similar ion- and voltage-dependencies when expressed in oocytes, both the B and C variants with an N-terminal autoinhibitory domain (AID) display reduced HCO_3^--induced currents (8). Injecting PIP_2 directly into an oocyte expressing NBCe1-C stimulates the mean HCO_3^--induced outward current by approximately 2.5 fold (26). PIP_2 injection also stimulates NBCe1-B, but has little effect on the activity of NBCe1-A with a different N terminus. The A variant compared to the B and C variants might have a much higher apparent affinity for PIP_2, and therefore be maximally active by endogenous PIP_2. Alternatively, the AID of the B and C variants might be "masked" by PIP_2 binding following injection. Further studies are required to assess if decreases in PIP_2 will inhibit NBCe1 activity.

Another important question is: What is the mechanism by which PIP_2 stimulates NBCe1 activity? As described above, PIP_2 typically binds to a stretch of positively charged amino acids. Many members of the BT superfamily—including NBCe1 and the Na-driven Cl-HCO_3 exchanger (NDCBE)—contain a stretch of lysines near their carboxyl termini. In addition, a stretch of arginines near the amino terminus of the B and C variants, but not the A variant, is another candidate PIP_2 binding site. Further studies are required to assess and characterize any potential direct interaction between PIP_2 and NBCe1 variants. We cannot exclude the possibility that PIP_2 stimulation of NBCe1 may involve an intermediate PIP_2-binding protein or the activation of other signaling molecules. Although the mechanism of stimulation has yet to be elucidated, Ca^{2+} is not required because all of our solutions were Ca^{2+} free.

Rundown of NBCe1 Activity. The majority of NBCe1 rundown was likely due to Mg^{2+}-dependent phosphatase activity because the rundown was largely inhibited by removing bath Mg^{2+}, both in the presence or absence of vanadate and F^-. We hypothesize that the 5′ lipid phosphatase contributes to rundown by dephosphorylating PIP_2 to PIP. Our data are consistent with the following model of rundown in our experiments. NBCe1 activity is evident in the majority of macropatches following excision because of the presence of endogenous PIP_2 in the membrane. However, a subsequent dephosphorylation event by a Mg^{2+}-dependent phosphatase decreases PIP_2 levels shortly thereafter and subsequently decreases NBCe1 activity. Applying bath PIP_2 resurrects NBCe1 activity (Fig. 3*A*), and to a greater extent in many cases if more rundown has occurred (Fig. 3 *C* and *D*).

Other phosphatases may also be involved because some rundown was evident (*i*) with 0 Mg^{2+}/F^-/vanadate (Fig. 2*B*), and (*ii*) with longer exposures to PIP_2. In principle, some of the "rundown" could be explained by a decrease in NBC activity due to the buildup of transported substrates within an unstirred layer on the pipette side of the macropatch. However, such buildup would be expected to dissipate quickly due to the large volume of the pipette solution. Furthermore, this possibility does not explain observed rundown with repetitive HCO_3^- exposures where reverse transport activity upon removing bath HCO_3^- (Fig. 2*B*) would be expected to dissipate such ion buildups.

While removing bath Mg^{2+} inhibits NBCe1-A rundown, we have recently discovered that raising bath Mg^{2+} appears to inhibit NBCe1-A directly. We found that raising bath Mg^{2+} decreases the HCO_3^--induced inward current much faster than seen with rundown. In addition, subsequently reducing bath Mg^{2+} reverses the Mg^{2+}-induced inhibition—an effect that occurs in the absence of ATP or phosphorylating conditions (required to reverse a protein and/or lipid phosphatase effect), and in the absence of exogenous PIP_2 (required to reverse a 5′ lipid phosphatase effect). In support of our findings, Yamaguchi and Ishikawa (27) recently reported that intracellular Mg^{2+} inhibits cloned NBCe1-B expressed in mammalian cells.

Physiological Significance of PIP_2-induced Stimulation of NBCe1. Phospholipids such as PIP_2 are powerful signaling molecules for many cellular processes. In the kidney, PIP_2 signaling will likely work in concert with hormones such as Ang II and messenger systems involving G proteins and PKC to regulate HCO_3^- reabsorption. In the nervous system, PIP_2-associated pH changes are likely to influence other PIP_2 targets such as M (KCNQ)-type K^+ channels that modulate neuronal excitability (28). In fact, such pH modulation may contribute to the specificity of PIP_2-mediated signaling—a topic of considerable interest in the lipid field (29). Finally, because the (re)generation of PIP_2 is ATP dependent, hypoxia/anoxia and ischemic conditions will lower PIP_2 levels. Subsequent inhibition of acid-extruding NBCe1s would be expected to contribute to the well-recognized intracellular acidosis associated with such energy-deficient pathologies (30–32).

Materials and Methods

Oocyte Isolation and NBCe1-A Expression. Oocytes were harvested from female *Xenopus laevis* frogs as previously described (8, 33). Segments of the ovarian lobe were harvested, teased apart into small pieces, and subjected to colla-

genase digestion. Dissociated stage-V/VI oocytes were washed and incubated at approximately 18 °C in sterile ND96 media supplemented with 10 mM Na-pyruvate and 10 mg/mL gentamycin (Mediatech).

Rat NBCe1-A was subcloned into the *Xenopus* oocyte expression vector pTLNII (34, 35). The vector was linearized with *Mlu* I and the cDNA transcribed using the SP6 transcription kit (Ambion). cRNA was purified with the RNeasy kit (Qiagen). Approximately 50 nL RNase-free H_2O or a solution containing cRNA was injected into an oocyte using a ''Nanoject II'' microinjector (Drummond Scientific). Experiments were performed at least 2 days after injection.

Electrophysiology. Macropatch studies were performed using the technique described by Hilgemann (23) and modified by our laboratory (8). Patch pipettes were pulled from N-51-A borosilicate glass capillaries (Drummond) using a PC-10 micropipette puller (Narishige), and then processed further using a custom-assembled microforge system. Tips gently broken to 10–12 μm were plunged into a bead of melted 8161 Corning glass (Warner Instruments) fixed to a heated 30-gauge, MF-9 platinum wire (Technical Products International). Upon cooling, the wire retracted to break the tip of the pipette. This process was repeated until an approximate 14-μm diameter pipette tip ($\approx$4 MΩ) was obtained.

An oocyte was shrunken in a hypertonic solution and the vitelline membrane removed with forceps to access the plasma membrane. Experiments were performed at room temperature ($\approx$22 °C) in a flow-through chamber on the stage of an inverted DMIRB microscope (Leica) as previously described (8). Exchange of bath solutions was achieved using a VC-6 perfusion valve control system (Warner Instruments) converging onto either one 8-port manifold or 2 such manifolds upstream of a SF-77B perfusion fast-step with 2 adjacent delivery lines (Warner Instruments) (36). Currents were obtained with an Axon Instruments Axopatch 200B patch-clamp amplifier (Molecular Devices), and digitized with an Axon Instruments Digidata-1321A interface (Molecular Devices). Axon Instruments pClamp 8.2 software (Molecular Devices) was used for data acquisition and analysis. In general, leak currents across patches in the ND96 bath solution were minimal based on total current measurements near 0. For data analysis and presentation purposes, baseline currents at the beginning of experiments were often set to 0.

Solutions. The standard ND96 solution used for incubating oocytes contained (in mM): 96 NaCl, 2 KCl, 1 $MgCl_2$, 1.8 $CaCl_2$, 5 HEPES, and NaOH to pH 7.5. The hyperosmotic solution contained (in mM): 220 *N*-methyl-D-glucammonium (NMDG)-aspartate, 2 $MgCl_2$, 10 EGTA, 10 HEPES, and $NMDG^+$ to pH 7.2. Ion-channel activity was minimized by using 0 K^+, 0 Ca^{2+}, low Cl^- (2 mM) solutions. The pipette solution contained (in mM): 96 NMDG-cyclamate, 1 $MgCl_2$, 3 EGTA, 5 HEPES, 10 NaOH, and cyclamic acid to pH 7.5. The ND96 solution used in recordings contained (in mM): 96 Na-cyclamate, 2 HCl, 3 EGTA, 5 HEPES, 2 (or 3) $Mg(OH)_2$, 8 (or 7) NaOH, and cyclamic acid to pH 7.5. For the 5% CO_2/33 mM HCO_3^- solution (pH 7.5), 33 mM Na-cyclamate was replaced with an equimolar amount of $NaHCO_3$, and the solution was equilibrated with 5% CO_2/balance O_2. Na^+-free solutions were made by replacing Na^+ with either $NMDG^+$ or Li^+.

One millimolar stock solutions of PIP_2 and 50 mM stock solutions of poly-D-lysine were prepared in deionized water and stored at -20 °C. PIP_2 was obtained from either Echelon Biosciences or Avanti Polar Lipids. All other chemicals were obtained from Sigma.

Statistics. Data are reported as mean $\pm$ standard error of the mean (SEM). Levels of significance were assessed using either the paired or unpaired Student's *t* test, and $P < 0.05$ was considered significant. Linear regression and comparisons of fits were performed using GraphPad Prism 5 (GraphPad Software).

ACKNOWLEDGMENTS. We thank Dr. Chou-Long Huang (Department of Medicine, University of Texas Southwestern Medical Center at Dallas) for providing guidance in using the macropatch technique. This work was supported by American Heart Association, Southeast Affiliate grant 0755255B (M.O.B.) and National Institutes of Health research grant R01 NS046653 (M.O.B.)

1. Romero MF, Hediger MA, Boulpaep EL, Boron WF (1997) Expression cloning and characterization of a renal electrogenic Na^+/HCO_3^- cotransporter. *Nature* 387:409–413.
2. Romero MF, Fulton CM, Boron WF (2004) The SLC4 Family of HCO_3^- transporters. *Pflügers Arch* 447:495–509.
3. Gross E, et al. (2003) Phosphorylation-induced modulation of pNBC1 function: Distinct roles for the amino- and carboxy-termini. *J Physiol* 549:673–682.
4. Gross E, et al. (2001) Phosphorylation of Ser^{982} in the sodium bicarbonate cotransporter kNBC1 shifts the HCO_3^-:Na^+ stoichiometry from 3:1 to 2:1 in murine proximal tubule cells. *J Physiol* 537:659–665.
5. Muller-Berger S, Ducoudret O, Diakov A, Frömter E (2001) The renal Na^+-HCO_3^- cotransporter expressed in *Xenopus laevis* oocytes: Change in stoichiometry in response to elevation of cytosolic Ca^{2+} concentration. *Pflügers Arch* 442:718–728.
6. Heyer M, Muller-Berger S, Romero MF, Boron WF, Frömter E (1999) Stoichiometry of the rat kidney Na^+-HCO_3^- cotransporter expressed in *Xenopus laevis* oocytes. *Pflügers Arch* 438:322–329.
7. Perry C, BlaineJ, Le H, Grichtchenko II (2006) PMA- and ANG II-induced PKC regulation of the renal Na^+-HCO_3^- cotransporter (hkNBCe1). *Am J Physiol Renal Physiol* 290:F417–F427.
8. McAlear SD, Liu X, Williams JB, McNicholas-Bevensee CM, Bevensee MO (2006) Electrogenic Na/HCO_3 cotransporter (NBCe1) variants expressed in *Xenopus* oocytes: Functional comparison and roles of the amino and carboxy termini. *J Gen Physiol* 127:639–658.
9. Shirakabe K, et al. (2006) IRBIT, an inositol 1,4,5-trisphosphate receptor-binding protein, specifically binds to and activates pancreas-type Na^+-HCO_3^- cotransporter 1 (pNBC1). *Proc Natl Acad Sci USA* 103:9542–9547.
10. Hilgemann DW, Feng S, Nasuhoglu C (2001) The complex and intriguing lives of PIP2 with ion channels and transporters. *Sci STKE* 2001:RE19.
11. Hilgemann DW, Ball R (1996) Regulation of cardiac Na^+,Ca^{2+} exchange and K_{ATP} potassium channels by PIP_2. *Science* 273:956–959.
12. Aharonovitz O, et al. (2000) Intracellular pH regulation by Na^+/H^+ exchange requires phosphatidylinositol 4,5-bisphosphate. *J Cell Biol* 150:213–224.
13. Fuster D, Moe OW, Hilgemann DW (2004) Lipid- and mechanosensitivities of sodium/hydrogen exchangers analyzed by electrical methods. *Proc Natl Acad Sci USA* 101:10482–10487.
14. Wu J, McNicholas-Bevensee CM, Bevensee MO (2007) Phosphatidylinositol 4,5-bisphosphate (PIP2) stimulates the electrogenic Na/bicarbonate cotransporter NBCe1-A *FASEB J* 21:916.13.
15. Sciortino CM, Romero MF (1999) Cation and voltage dependence of rat kidney electrogenic Na^+-HCO_3^- cotransporter, rkNBC, expressed in oocytes. *Am J Physiol* 277:F611–F623.
16. Liu X, Williams JB, Sumpter BR, Bevensee MO (2007) Inhibition of the Na/bicarbonate cotransporter NBCe1-A by diBAC oxonol dyes relative to niflumic acid and a stilbene. *J Membr Biol* 215:195–204.
17. Choi I, Romero MF, Khandoudi N, Bril A, Boron WF (1999) Cloning and characterization of a human electrogenic Na^+-HCO_3^- cotransporter isoform (hhNBC). *Am J Physiol* 276:C576–C584.
18. McNicholas CM, Wang W, Ho K, Hebert SC, Giebisch G (1994) Regulation of ROMK1 K^+ channel activity involves phosphorylation processes. *Proc Natl Acad Sci USA* 91:8077–8081.
19. McNicholas CM, Yang Y, Giebisch G, Hebert SC (1996) Molecular site for nucleotide binding on an ATP-sensitive renal K^+ channel (ROMK2). *Am J Physiol* 271:F275–F285.
20. Takano M, Noma A (1993) The ATP-sensitive K^+ channel. *Prog Neurobiol* 41:21–30.
21. Pochynyuk O, Tong Q, Staruschenko A, Ma HP, Stockand JD (2006) Regulation of the epithelial Na^+ channel (ENaC) by phosphatidylinositides. *Am J Physiol Renal Physiol* 290:F949–F957.
22. Hilgemann DW (1990) Regulation and deregulation of cardiac Na^+-Ca^{2+} exchange in giant excised sarcolemmal membrane patches. *Nature* 344:242–245.
23. Hilgemann DW (1995) in *Single Channel Recording*, eds Sackmann B, Neher E (Plenum Press, New York), pp 307–327.
24. Nelson N, Sacher A, Nelson H (2002) The significance of molecular slips in transport systems. *Nat Rev* Mol Cell Biol 3:876–881.
25. Choi I, Aalkjaer C, Boulpaep EL, Boron WF (2000) An electroneutral sodium/bicarbonate cotransporter NBCn1 and associated sodium channel. *Nature* 405:571–575.
26. Wu J, Liu X, Thornell IM, Bevensee MO (2009) Phosphatidylinositol 4,5-bisphosphate stimulation of electrogenic Na/bicarbonate cotransporter NBCe1 variants expressed in *Xenopus laevis* oocytes. *FASEB J* 22:800.13.
27. Yamaguchi S, Ishikawa T (2008) The electrogenic Na^+-HCO_3^- cotransporter NBCe1-B is regulated by intracellular Mg^{2+}. *Biochem Biophys Res Commun* 376:100–104.
28. Zaika O, et al. (2006) Angiotensin II regulates neuronal excitability via phosphatidylinositol 4,5-bisphosphate-dependent modulation of Kv7 (M-type) K^+ channels. *J Physiol* 575:49–67.
29. Gamper N, Shapiro MS (2007) Target-specific PIP_2 signalling: How might it work? *J Physiol* 582:967–975.
30. Siesjö BK, Katsura K, Kristian T (1996) Acidosis-related damage. *Adv Neurol* 71:209–233.
31. Tombaugh GC, Sapolsky RM (1993) Evolving concepts about the role of acidosis in ischemic neuropathology. *J Neurochem* 61:793–803.
32. Yao H, Haddad GG (2004) Calcium and pH homeostasis in neurons during hypoxia and ischemia. *Cell Calcium* 36:247–255.
33. McAlear SD, Bevensee MO (2006) A cysteine-scanning mutagenesis study of transmembrane domain 8 of the electrogenic sodium/bicarbonate cotransporter NBCe1. *J Biol Chem* 281:32417–32427.
34. Romero MF, Fong P, Berger UV, Hediger MA, Boron WF (1998) Cloning and functional expression of rNBC, an electrogenic Na^+-HCO_3^- cotransporter from rat kidney. *Am J Physiol* 274:F425–F432.
35. Romero MF, Kanai Y, Gunshin H, Hediger MA (1998) Expression cloning using *Xenopus laevis* oocytes. *Methods Enzymol* 296:17–52.
36. McNicholas-Bevensee CM, et al. (2006) Activation of gadolinium-sensitive ion channels in cardiomyocytes in early adaptive stages of volume overload-induced heart failure. *Cardiovasc Res* 72:262–270.